JOURNAL OF MATERIALS SCIENCE 16 (1981) 3006–3012

A comparative study of precipitation at interphase boundaries in Fe–Cu–Ni and Fe–Au–Ni alloys

R. A. RICKS
Department of Metallurgy and Materials Science, University of Cambridge, Pembroke Street, Cambridge, UK

This paper reports the results of a comparative study on the formation of interphase boundary nucleated precipitates in an Fe–2 wt% Cu–2 wt% Ni and an Fe–4 wt% Au–2 wt% Ni alloy. High-speed dilatometry has been used to determine the kinetics of the austenite–ferrite transformation in these alloys and the resultant microstructures have been investigated using both light microscopy and transmission electron microscopy. The differences in precipitate morphology observed are discussed in terms of the reaction kinetics of the two alloys.

1. Introduction

The formation of carbide precipitates on a migrating austenite–ferrite interphase boundary during the decomposition of austenite has been studied extensively in steels and has received many excellent reviews [1, 2]. Recently this interphase precipitation reaction has also been observed in carbon-free iron-based alloys, in which the precipitating phase was ϵ-Cu [3]. Although the reaction was found to be essentially similar for both carbide and ϵ-Cu precipitation, only particulate copper precipitates were observed, whereas in steels a fibrous carbide morphology is commonly seen.

One major difference between the precipitation reactions involving alloy carbides and ϵ-Cu in steels is that copper is known to undergo a pre-precipitation or clustering stage, where b c c copper clusters are formed in the ferrite matrix prior to the formation of f c c copper precipitates [4]. This is thought to be a consequence of the low strain energy involved, since the atomic sizes of the iron and copper atoms only differ by approximately 0.3% [5]. The consequences of this pre-precipitation clustering stage result in a lowering of the nucleation energy barrier allowing the formation of a homogeneous dispersion of ϵ-Cu precipitates in the ferrite [6].

In contrast the atomic sizes of iron and gold differ by 12.6% and therefore the precipitation of Au from supersaturated ferrite does not involve any pre-precipitation stage [5]. Thus, the precipitation of Au in Fe is similar to the precipitation of the majority of alloy carbides in steels, where the high nucleation barrier favours precipitation on grain boundaries and dislocations.

The purpose of this paper is to investigate the effect of strain energy in the formation of precipitation on interphase boundaries in an Fe–2 wt% Cu–2 wt% Ni alloy and an Fe–4 wt% Au–2 wt% Ni alloy. These compositions were chosen to ensure approximately equivalent supersaturations of the ferrite in both alloys in the isothermal transformation termperature range thus ensuring that any change in precipitation behaviour should be associated with the difference in strain energy.

2. Experimental procedure

The alloys used in this investigation were made from high-purity base elements, melted in an argon arc furnace to give the following compositions:

Actual
Fe–1.9 wt% Cu–1.9 wt% Ni
Fe–3.8 wt% Au–2.0 wt% Ni

Nominal
Fe–2 wt% Cu–2 wt% Ni
Fe–4 wt% Au–2 wt% Ni.

0022–2461/81/113006–7$02.70/0

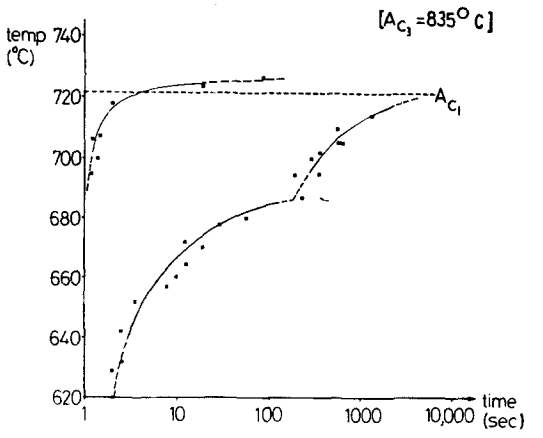

Figure 1 Dilatometrically determined TTT diagram for the Fe–2 wt% Cu–2 wt% Ni alloy showing the reaction start and finish curves and the experimentally determined Ac_1, Ac_3 temperatures.

Each alloy was homogenized at 1200° C for 72 h prior to heat treatment in a de-oxidized tin bath pre-set at the required transformation temperature. Optical microscopy of the heat-treated specimen material was performed using a Zeiss Universal microscope with an etchant of 2% nital. Specimens for electron microscopy were prepared from discs, 3 mm in diameter, punched from the heat-treated material, using a twin-jet electropolisher with an electrolyte consisting of 10 vol% perchloric acid, 20 vol% glycerol and 76 vol% ethanol. All electron microscopy was performed on a Philips EM 300 operating at 100 kV.

The time–temperature–transformation (TTT) curves for the two alloys were obtained using a high-speed dilatometer employing helium gas as a quenchant. Specimens for dilatometry were in the form of hollow rods, 15 mm long, 3 mm diameter, with a wall thickness of 0.5 mm. Using specimens of these dimensions quench rates of up to 300° C sec^{-1} could be attained.

3. Results

3.1. Fe–2 wt% Cu–2 wt% Ni alloy

The austenite–ferrite transformation in this alloy has been studied previously [3] and only a brief outline of the reaction kinetics and ferrite morphologies obtained will be given here. Fig. 1 shows the dilatometrically determined TTT curve for this alloy. The pronounced discontinuity observed in the reaction finish curve was shown by Ricks *et al.* [3] to be due to a changeover in solute diffusion paths at the temperature of the discontinuity. Thus, above approximately 690° C the ferrite was often observed to contain a dispersion of interfacial nucleated ϵ-Cu precipitates (Fig. 2), the formation of which involved the diffusion of copper in the interphase boundary. Below 690° C only supersaturated ferrite was observed, which involves only transboundary diffusion of copper. The morphology of the ϵ-Cu dispersions in the ferrite formed above 695° C could consist of either planar sheets of precipitates (Fig. 2a) which most probably formed on

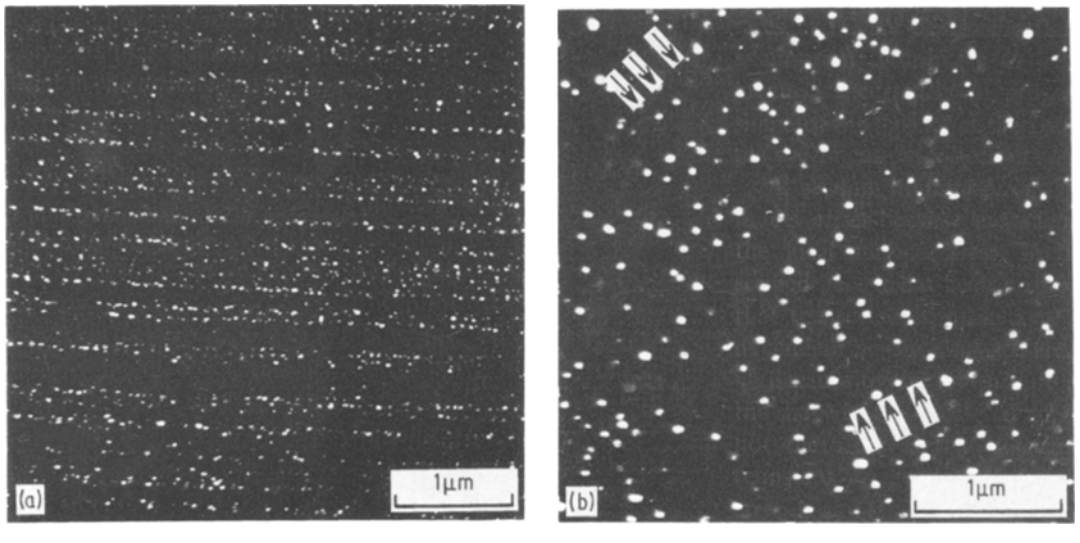

Figure 2 ϵ-Cu centred dark-field transmission electron micrographs showing (a) planar sheets of precipitates, formed on low energy interphase boundaries, and (b) irregular curved sheets of precipitates (arrowed), formed on high energy boundaries.

partially coherent low-energy interphase boundaries, or curved sheets of precipitates (Fig. 2b) which formed on high-energy interphase boundaries.

3.2. Fe–4 wt% Au–2 wt% Ni alloy

The dilatometrically determined TTT curve for this alloy is shown in Fig. 3. Compared with that of the copper-bearing alloy (Fig. 1) the ferrite reaction is seen to nucleate more slowly in this alloy and a discontinuity in the reaction start curve was detected at about 690° C. The extremely sluggish nature of the ferrite reaction above this temperature prohibited the acquisition of accurate reaction finish times; hence, it could not be ascertained whether a similar discontinuity existed in the reaction finish curve.

Examination of specimens transformed above and below the temperature of the discontinuity (~690° C) by light microscopy showed that in both temperature regimes equiaxed ferrite was formed (Fig. 4). However, examination at higher magnification revealed that the ferrite formed at temperatures above 690° C contained sheets of precipitates (Fig. 5). This observation was confirmed by electron microscopy, which also showed that the precipitate dispersions could have several morphologies, namely,

(i) approximately planar sheets of Au precipitates (Fig. 6a),

(ii) curved, irregular sheets of Au precipitates (Fig. 6b),

(iii) fibrous precipitation of Au (Fig. 6c).

Electron diffraction evidence suggested that in

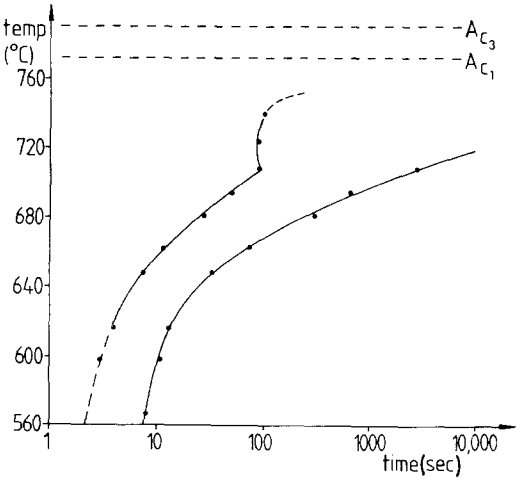

Figure 3 Dilatometrically determined TTT diagram for the Fe–4 wt% Au–2 wt% Ni alloy.

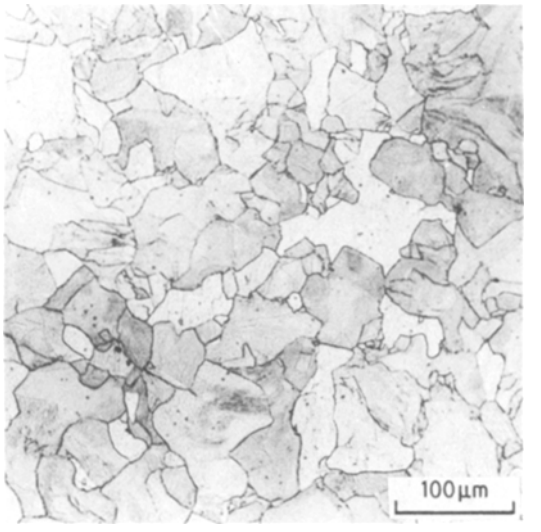

Figure 4 Light optical micrograph showing equiaxed ferrite formed by isothermal transformation at 720° C for 2 h.

all cases the orientation relationship between the ferrite and the gold precipitates was consistent with Baker–Nutting orientation relationship [7], i.e.

$$(0\,0\,1)_{Au} \,//\, (0\,0\,1)_{Fe}$$
$$[1\,1\,0]_{Au} \,//\, [1\,0\,0]_{Fe},$$

as originally observed by Higgins and Wilkes (8). This orientation relationship is to be expected since the lattice mismatch between iron and gold is approximately the same as that between iron

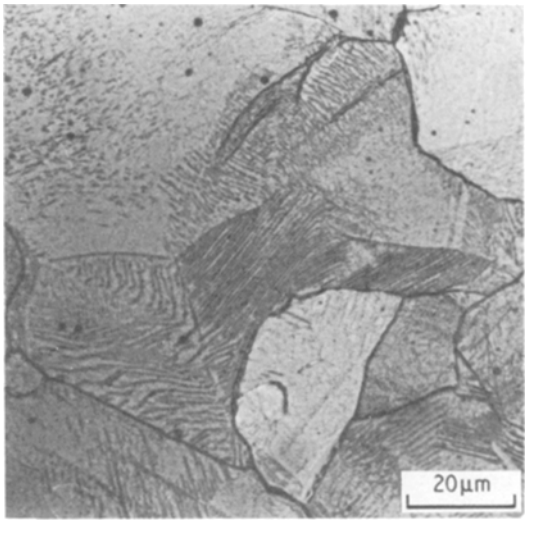

Figure 5 Light optical micrograph showing the banded dispersion of the Au precipitates in equiaxed ferrite formed by isothermal transformation at 735° C for 1 h.

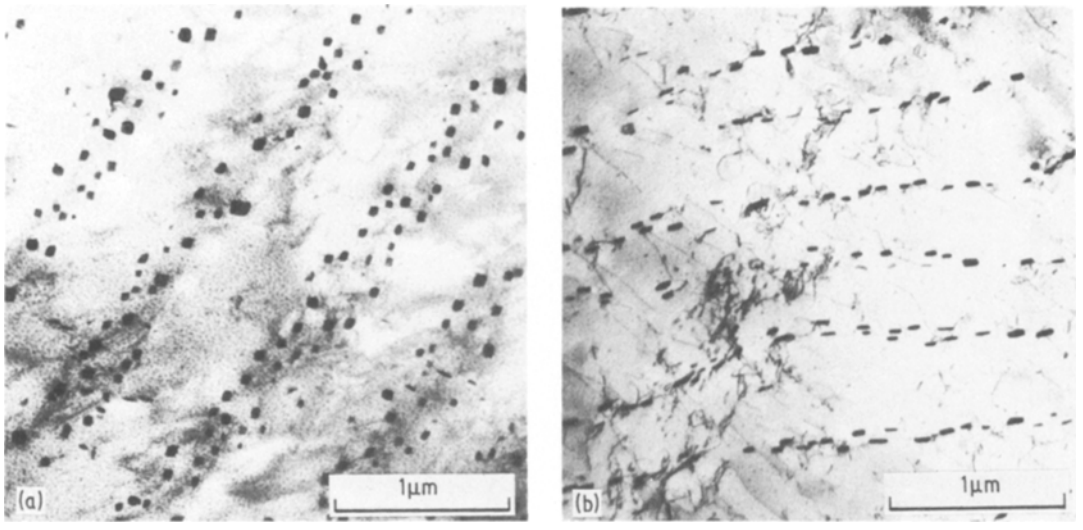

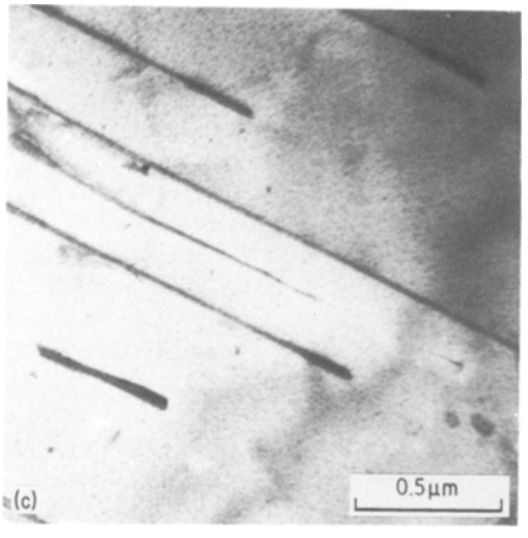

Figure 6 Bright-field transmission electron micrographs showing the Au precipitate morphology formed by isothermal transformation at 720° C for 2 h. (a) Approximately planar sheets of Au precipitates, (b) irregular curved sheets of precipitates and (c) fibrous precipitates.

and the MC carbides which also obey this orientation relationship.

The planar sheets of gold precipitates (Fig. 6a) imply that the interphase boundary on which they were formed was low-energy in nature and thus this type of precipitate dispersion is directly analogous to that observed in the Fe–2 wt% Cu–2 wt% Ni alloy (Fig. 2a). Similarly, the curved, irregular sheets shown in Fig. 6b are most probably associated with the migration of a high-energy interphase boundary, in the same manner as the formation of the equivalent precipitate dispersion in the Fe–2 wt% Cu–2 wt% Ni alloy. In contrast to the ϵ-Cu precipitates however, which were approximately spherical in shape, the gold precipitates were plate-shaped and had a distinct habit plane with the ferrite. Hornbogen [5] has shown that this habit plane is close to $(1\,0\,0)_\alpha$ and of particular interest is that the precipitates which nucleate on the austenite–ferrite interface generally adopt the same habit plane and crystallographic orientation (Fig. 7). Occasionally a few precipitates were observed to choose an alternative habit plane (Fig. 8) which usually caused a "step" in the plane of the sheet of precipitates. This will be discussed further in Section 4. In all cases the observed particulate precipitate dispersions in the Fe–4 wt% Au–2 wt% Ni alloy were much coarser than those observed in the Fe–2 wt% Cu–2 wt% Ni alloy.

The fibrous precipitate morphology observed in this alloy has no direct counterpart in the Fe–Cu–Ni alloy. This type of precipitation was less commonly observed than the two particulate dispersions, and occasionally both could be observed together (Fig. 9). This latter observation implies that the same interphase boundary can form either a particulate or fibrous precipitate colony.

Electron microscopy of specimens transformed below 690° C revealed that the ferrite was formed supersaturated with respect to gold, although subsequent precipitation of gold on dislocations and grain boundaries rapidly occurred (Fig. 10).

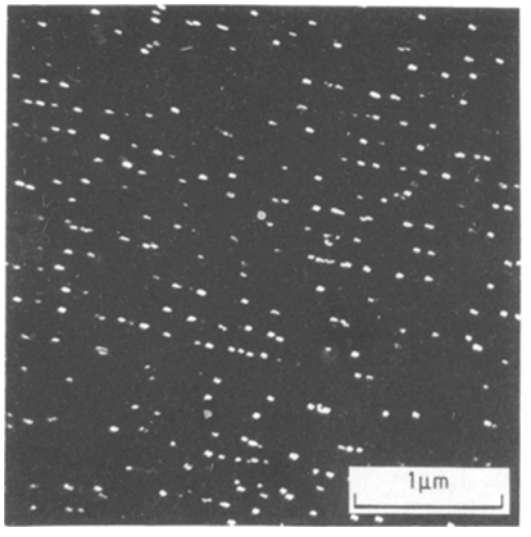

Figure 7 Au-centred dark-field transmission electron micrograph showing the univariance in orientation relationship of the precipitates in any colony.

4. Discussion

The growth rate of ferrite in alloys which form colonies of interphase precipitation will be a sensitive function of such parameters as the diffusivity of the solute and the nucleation rate of the precipitating phase on the interphase boundary. In the Fe–Cu–Ni alloy, Ricks *et al.* [3] concluded that in the temperature range where ϵ-Cu interphase precipitation was formed (approximately 725 to 695° C) the diffusion path taken by the solute (Cu) was confined to the interphase boundaries. Subsequent investigations [9] concerning the use of scanning transmission electron microscopy/energy dispersive spectroscopy (STEM/EDS) analysis have shown that within the spatial resolution of the technique (30 nm), no volume diffusion in austenite occurs in these alloys. In view of the similarities, both kinetic and microstructural, which exist in the two alloys investigated here, it seems likely that solute diffusion is indeed confined to the interphase boundary.

Very little detailed information exists concerning solute diffusivities in interphase boundaries and, furthermore, the diffusivity in a migrating interphase boundary is likely to be dissimilar to that in a static boundary. It is, therefore, not possible to accurately calculate the growth rate of an interphase boundary which is controlled by the diffusion of solute atoms within the boundary. Thus it is impossible to state unambiguously whether the sluggish ferrite growth rate observed in both alloys at high temperatures was controlled by solute diffusion or the nucleation rate of precipitates, which periodically relieves the build up of solute within the boundary.

Despite this, some conclusions can be drawn from the results of this investigation. The growth rate of ferrite at high temperatures in the Fe–4 wt% Au–2 wt% Nt alloy is approximately an order of magnitude slower than in the Fe–2 wt% Cu–2 wt% Ni alloy, at the same temperature (cf. Figs 1 and 3). Furthermore, the resultant precipitate dispersions in the gold-bearing alloy were much coarser than in the copper alloy. This suggests, even if preferential growth of precipitates

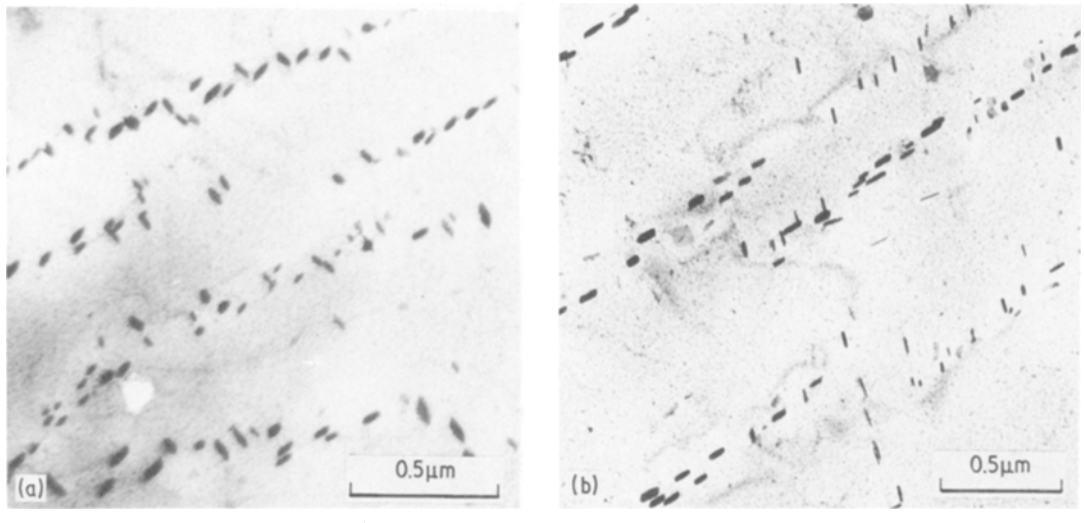

Figure 8 Bright-field transmission electron micrographs showing colonies of interphase Au precipitates in which at least two precipitate habit planes are observed. Isothermally transformed at 735° C for 1 h.

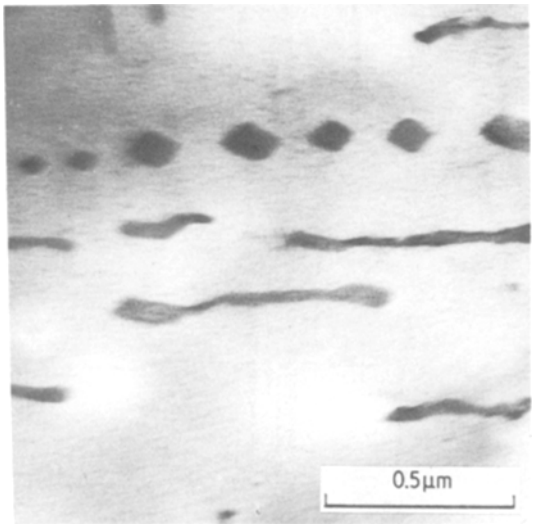

Figure 9 Bright-field transmission electron micrograph showing concommitant formation of particulate and fibrous precipitates of Au. Isothermally transformed at 735° C for 1 h.

is allowed for, that the nucleation rate of the gold precipitates on the interphase boundary was lower than that of the copper precipitates. This observed difference in precipitate dispersion morphology may imply that the pre-precipitation behaviour known to be associated with the formation of copper precipitates during ageing treatments could influence the ability of a migrating interphase boundary to nucleate interphase precipitation of

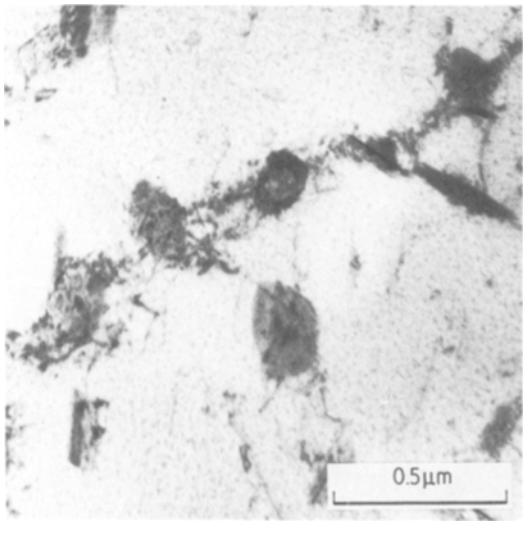

Figure 10 Bright-field transmission electron micrograph showing large plate-shaped Au precipitates produced by the decomposition of supersaturated ferrite formed by isothermal transformation at 650° C for 100 sec.

ϵ-Cu. The larger atomic size associated with gold atoms would prevent any pre-precipitation enhancement of nucleation in the Fe–4 wt% Au–2 wt% Ni alloy, and thus there would be greater difficulty involved in forming a critical nucleus of a gold precipitate on the boundary. This hypothesis is substantiated by the observation of gold fibres in the Fe–4 wt% Au–2 wt% Ni alloy which indicates that under certain conditions it is more favourable for the boundary to add solute to existing precipitates to form fibres as it migrates, rather than nucleate new precipitates. The observation of both particulate and fibrous precipitates in the same colony (Fig. 10) suggests that the local conditions at the interphase boundary greatly influence the final precipitate morphology. The enhancement in nucleation rate which would be associated with a pre-precipitation stage in the formation of ϵ-Cu precipitates could also explain the complete lack of any fibrous precipitates observed in the Fe–2 wt% Cu–2 wt% Ni alloy.

It is interesting to note that the same conditions of slow ferrite growth rate and low precipitate nucleation rate are found at high transformation temperatures in alloy steels. Similarly, fibrous carbide morphologies are also predominant in many alloy steels at these high transformation temperatures [1, 2, 10]. Furthermore, as the transformation temperature is decreased, which, above the "nose" of the TTT diagram reduces the total transformation time and increases nucleation rates, particulate interphase precipitation is predominantly observed [11].

The univariance of the precipitate colonies formed in the Fe–4 wt% Au–2 wt% Ni alloy is presumably a result of the influence of the local boundary habit plane at the time of nucleation (see [12]). Howell *et al.* [13] observed that for precipitate planes which were related to the ferrite by a Kurdjumov–Sachs [14] orientation relationship (e.g. ϵ-Cu), the univariance of interphase precipitate colonies could be a result of the three-phase crystallography, generated across interfaces separating Kudjumov–Sachs [14] related austenite and ferrite. Since the gold precipitates were not observed to obey this Kurdjumov–Sachs [14] orientation relationship, then a three-phase crystallography is not possible and therefore cannot control the selection of orientation or habit plane of the precipitates. Supportive evidence for the influence of the habit plane of the boundary upon the habit plane selection of the precipitate comes

from Fig. 8, which shows that occasionally the curvature of the interphase boundary is such that a precipitate may choose two different habit planes depending on the *local* habit plane of the boundary.

Finally, the discontinuity in the reaction start curve of the TTT diagram for the Fe–4 wt% Au–2 wt% Ni alloy may be due to a segregation of gold atoms to the austenite grain boundaries which may inhibit ferrite nucleation as suggested by Shama and Purdy [15]. As the temperature of transformation is decreased the driving force for the ferrite reaction will increase and at some critical temperature, given by the temperature of the discontinuity, their inhibiting effect will be overcome.

5. Summary and conclusions

The results of this investigation have shown the following:

(a) The kinetics of the austenite–ferrite reaction in both Fe–4 wt% Au–2 wt% Ni and Fe–2 wt% Cu–2 wt% Ni alloys at low undercoolings is sufficiently low to allow the formation of interphase precipitation of Au and Cu, respectively.

(b) At lower transformation temperatures the driving force for the ferrite reaction increases sufficiently to prevent solute diffusion occurring in the interphase boundary. This results in the formation of supersaturated ferrite which may decompose at the temperature of transformation.

(c) The difficulty associated with the formation of nuclei of gold precipitates which results from the high strain energy associated with gold atoms in iron could account for the coarse precipitate dispersion observed in the Fe–4 wt% Au–2 wt% Ni alloy. Furthermore the observation of fibrous gold precipitates may be explained in terms of the low precipitate nucleation rate on interphase boundaries in this alloy.

References

1. R. W. K. HONEYCOMBE, *Met. Trans. A* 7A (1976) 915.
2. *Idem, Met. Sci.* **14** (1980) 201.
3. R. A., RICKS, P. R. HOWELL and R. W. K. HONEYCOMBE, *Met. Trans. A* **10A** (1979) 1049.
4. S. R. GOODMAN, S. S. BRENNER and J. R. LOW, *ibid.* **4** (1973) 2363.
5. E. HORNBOGEN, *Acta Met.* **10** (1962) 525.
6. E. HORNBOGEN and R. C. GLENN, *Trans. ASM – AIME* **218** (1960) 1064.
7. R. G. BAKER and J. NUTTING, Iron and Steel Institute Report No. 64 (Iron and Steel Institute, London, 1959) p. 1.
8. J. HIGGINS and P. WILKES, *Phil. Mag.* **25** (1972) 599.
9. R. A. RICKS, Proceedings of the 7th European Congress on Electron Microscopy, 1980, The Hague, Netherlands, Vol. 3, edited by P. Brederoo and V. E. Cossiett, p. 184.
10. D. V. EDMONDS, *J. Iron Steel Inst.* **210** (1972) 363.
11. J. V. BEE, P. R. HOWELL and R. W. K. HONEYCOMBE, *Met. Trans. A* **10A** (1979) 1207.
12. A. T. DAVENPORT, F. G. BERRY and R. W. K. HONEYCOMBE, *Met. Sci.* **2** (1968) 104.
13. P. R., HOWELL, R. A. RICKS, J. V. BEE and R. W. K. HONEYCOMBE, *Phil. Mag.* **41** (1980) 165.
14. G. KURDJUMOV and G. SACHS, *Z. Phyzik* **64** (1930) 325.
15. R. C. SHAMA, and G. R. PURDY, *Met Trans.* **4** (1973) 2303.

Received 16 February and accepted 6 April 1981.